Journal of Nuclear Medicine, published on June 29, 2018 as doi:10.2967/jnumed.118.211698

VT Substrate Characteristics: Insights from Multi-modality Structural and Functional Imaging of the VT Substrate Using CMR Scar, ^{123}I-mIBG-SPECT Innervation and Bipolar Voltage

Short running title: VT Substrate Characteristics

Hasan Imanli*,MD[1,2], Kiddy L. Ume*,MD[1,2], Jean Jeudy,MD[1,3], Tamunoinemi Bob-Manuel,MD[1,2], Mark F. Smith,PhD[1,3], Wengen Chen,MD,PhD[1,3], Mohammed Abdulghani,MD[1,2], Yousra Ghzally,MD[1,2], Jagat Bandhu Mahat,MBBS[,2], Refael Itah,MD,PhD[4], Alejandro Restrepo,MD[1,2], Vincent Y. See,MD[1,2], Stephen Shorofsky,MD,PhD[1,2], Vasken Dilsizian,MD[1,3], Timm Dickfeld,MD,PhD[1,2]

**H. Imanli and K.L. Ume contributed equally to this work*

Maryland Arrhythmia and Cardiology Imaging Group (MACIG)[1], Division of Cardiology, Department of Medicine[2], Department of Diagnostic Radiology and Nuclear Medicine[3], Baltimore, MD and Biosense Webster, Haifa, Israel[4]

Word Count: 4982

Corresponding Author:

Timm Dickfeld, MD, PhD

Division of Cardiology

University of Maryland School of Medicine

22 S Greene St

Baltimore, MD, 21201, USA

Email: tdickfel@som.umaryland.edu

Phone: (410) 328-6056 Fax: (410) 328-2062

First Authors:

Hasan Imanli, MD

himanli@som.umaryland.edu

(410) 328-7627

Kiddy L. Ume, MD

kume@som.umaryland.edu

ABSTRACT

Background – Post-Ischemic adaptation results in characteristic myocardial structural and functional changes of the VT(Ventricular Tachycardia) substrate. **Objective –** Compare myocardial structural/functional adaptation (late gadolinium-enhancement(LGE)/abnormal innervation) with detailed VT mapping data to identify regional heterogeneities of post-ischemic changes. **Methods –** Fifteen patients with ischemic cardiomyopathy and drug-refractory VT underwent LGE-Cardiac magnetic resonance imaging(CMR), ^{123}I-mIBG–SPECT and high-resolution bipolar voltage mapping to assess fibrosis(>3SD), abnormal innervation(<50% tracer uptake) and low-voltage areas(<1.5mV), respectively. 3D-reconstructed CMR/^{123}I-mIBG models were co-registered for further comparison. **Results** – Post-ischemic structural/functional adaptation in all three categories was similar in size (CMR scar 46.1cm^2[33.1–86.9cm^2] vs. ^{123}I-mIBG–SPECT abnormal innervation 47.8cm^2[40.5–68.1cm^2] vs. low-voltage area 29.5cm^2[24.5–102.6cm^2], p>0.05). Yet, any single modality underestimated the total VT substrate area, defined as abnormal in at least one of the three modalities (76.0cm^2[57.9-143.2cm^2]; p<0.001). Within the total VT substrate area, regions abnormal in all 3 modalities were most common (25.2%). However, significant parts of the VT substrate had undergone heterogeneous adaptation (abnormal in <3 modalities); most common categories were ‘abnormal innervation only’(18.2%), ‘CMR scar+abnormal innervation only’(14.9%) and ‘CMR scar only’(14.6%). All 14 VT channel/exit sites(0.88±0.74mV) localized to myocardium demonstrating CMR scar AND abnormal innervation. This specific tissue category accounted for 68.3% of the CMR scar and 31.2% of the total abnormal post-ischemic VT substrate. **Conclusion –** Structural/functional imaging demonstrates regional heterogeneities of the post-ischemic VT substrate not appreciated by any single modality alone. Co-existence of abnormal innervation and CMR scar may identify a state of particularly proarrhythmic adaptation and represent a potential novel target for VT ablation.

Keywords: multi-modality, cardiac imaging, innervation, ventricular tachycardia

ABREVIATION LIST

EAM=electroanatomic mapping

^{123}I-*m*IBG=^{123}I-Meta-Iodobenzylguanidine

VT=Ventricular Tachycardia

LGE-CMR=Late Gadolinium Enhancement-Cardiac Magnetic Resonance

SPECT=Single-Photon Emission Computed Tomography

3D=Three Dimensional

LV=Left Ventricle

RV=Right Ventricle

CMR-Sc=LGE-CMR Scar

ABNINNERV=^{123}I–*m*IBG abnormal innervation zone

LowVolt=low-voltage area <1.5mV

TotalVTSubstr=the total area of the VT substrate

INTRODUCTION

Intra-procedural electro-anatomic mapping (EAM) based on the catheter-based voltage measurements are used as the “gold standard” for electrophysiological substrate identification in ischemic cardiomyopathy. However, EAM is time-intensive, cannot completely represent complex intramural, three dimensional (3D) scar structures, and can result in mapping inaccuracies due to both suboptimal catheter contact and limited spatial resolution(*1*). Therefore, structural imaging assessing anatomic changes with Late Gadolinium Enhancement-Cardiac Magnetic Resonance imaging (LGE-CMR) or multi-detector Computed Tomography (CT) (*1-4*), and functional imaging assessing changes in cellular function such as metabolism/innervation using Fluorodeoxyglucose-Positron Emission Tomography (FDG-PET) (*5,6*), and ^{123}I-Metaiodobenzylguanidine (^{123}I-*m*IBG) Single-photon emission computed tomography (SPECT) (*7,8*) have both been investigated in order to better characterize the 3D Ventricular Tachycardia (VT) substrate.

Both structural and functional imaging demonstrated a good-to-moderate correlation to the voltage-defined VT substrate. However, there are small-to-moderate degrees of mismatch between structural imaging (CMR/CT) and functional imaging (FDG-PET/^{123}I-*m*IBG innervation) to electroanatomical map (EAM), respectively which suggest that post-ischemic adaptation may be a more complex, heterogeneous process affecting structural and functional properties of the VT substrate to a variable degree(*1,3,7-10*). A comparison of structural and functional imaging properties and their correlation to EAM/VT substrate data has not been performed previously.

Therefore, this single-center feasibility study sought to perform a comparison of structural imaging changes (CMR fibrosis) and functional imaging changes (^{123}I-mIBG innervation) with correlation to bipolar mapping data to provide novel insights into the regional adaptation of the post-ischemic VT substrate and identify imaging characteristics of VT channel/exit sites.

METHODS

STUDY PROTOCOLS AND PATIENT POPULATION. The study was designed as a single-center feasibility study of consecutive patients with ischemic cardiomyopathy scheduled for radiofrequency ablation for drug-refractory VT. Study protocols were approved by the University of Maryland Institutional Review Board and all subjects signed a written informed consent.

LGE-CMR ACQUISITION PROTOCOL. ECG-gated inversion recovery images were obtained with a 1.5-T scanner (Magnetom® Avanto; Siemens, Erlangen/Germany) during diastole 10-15 minutes after intravenous injection of 0.1mg/kg gadobenate dimeglumine. Short- and long-axis 2D (slice thickness: 8mm; no gap; inversion time: 250-350ms; repetition time: 725-950ms; echo time: 1- 4ms; flip angle: 25°) inversion recovery sequences were obtained after optimal nulling to assess LGE. When possible, a novel inversion preparation pulse with a wide inversion bandwidth of 2.4 kHz was employed to reduce metal artifact.

LGE-CMR IMAGE PROCESSING. The LGE-CMR images were exported as Digital Imaging and Communications in Medicine (DICOM) file format and processed with the CARTOSEG™ MR Segmentation Module (Biosense Webster, Diamond Bar, USA). Epi/endocardial borders of the LV were outlined in all sequential short-axis slices (Figs. 1A and 1B). Areas with metal artifact were manually traced and excluded from further analysis. The scar was defined as voxels with intensities greater than 3 standard deviations in a histogram-based analysis using a remote area of normal myocardium(*11,12*). Segmentation results were confirmed by an expert radiologist reader with >15 years of experience (J.J.).

^{123}I-MIBG SCINTIGRAPHY. Pre-procedural ^{123}I-mIBG SPECT images were obtained before VT ablation. Patients were administered 370MBq (10mCi) of ^{123}I-mIBG (GE Healthcare, Chicago, IL, USA) intravenously. SPECT imaging of the chest was performed using a dual-head gamma camera (SKYLight, Philips, Milpitas, CA, USA) 4h after injection, with minimum 30 projections/head, 20–30 seconds/projection, 64×64 matrix. Camera heads were equipped with

low-energy, high-resolution collimators, and all acquisitions were performed with a 20% energy window centered at the 159-keV photopeak of ^{123}I.

3D ^{123}I-MIBG CARDIAC MAP RECONSTRUCTION. 3D reconstructions of myocardial innervation were created using the Amira 5.4.2 software (Visage Imaging, San Diego, CA, USA). On each 2D ^{123}I-*m*IBG SPECT slice, areas of the abnormally innervated myocardium (<50% tracer uptake) were determined visually by two blinded, experienced cardiac nuclear medicine physicians (V.D. and W.C.) with a previously demonstrated <10% intra-/interobserver variability (*8*). Using the sequential 2D datasets, individual 3D innervation maps were created for each of the patients in the Amira environment (Figs. 1C and 1D). RV reconstruction was performed to correct for rotational errors during registration. The datasets were then converted to CARTO® 3 System readable mesh files using custom-made software (*7*).

VOLTAGE MAP AND VT ABLATION. LV voltage maps were created through a retrograde/transseptal approach using a filling threshold of <10mm and voltage settings of 0.5 to 1.5mV. Bipolar signals were filtered at 10-400Hz and were acquired during sinus rhythm or during ventricular pacing in patients with resynchronization therapy or pacemaker dependency. Any areas with a voltage <1.5mV were considered abnormal (*2,9,10,13*).

The ablation procedures were performed with a 3.5-mm open irrigated-tip catheter (THERMOCOOL® or SF/SMARTTOUCH™, Biosense, Diamond Barr, USA). Ablation targets were any clinical VT documented by 12-lead ECGs or presumed clinical VT defined by matching cycle length, far-field morphology and local electrogram-to-far-field electrogram relationship from Implantable cardioverter-defibrillator recordings. First, sustained monomorphic VT matching the clinical or presumed clinical VT was induced to obtain a current 12-lead ECG template. Second, pace map matches ≥11/12 leads with the longest stim-QRS were used to approximate the VT channel/exit(*14,15*). Third, entrainment/activation mapping was performed to the maximum degree tolerated after reinduction of the VT to confirm the anatomic location of the VT channel/exit

site, which was then used for further analyses (*14,15*). RF ablation was performed orthogonally to the defined channel using single, overlapping RF lesions (40-50W, 60s each). After the ablation, programmed electric stimulation with up to triple extrastimuli and shortest coupling interval of 200ms from at least 2 RV/LV sites was repeated and successful ablation was defined as the inability to induce the ablated clinical VT.

3-WAY COMPARISON AND ANALYSIS. The 3D CMR and MIBG maps were transferred to the clinical CARTO® 3 System using the CARTOMERGE® Module. These maps were co-registered with high-density voltage maps by obtaining multiple matching landmark pairs (superior/inferior RV septal insertion, mitral valve, apex and additional assessment of ascending aorta) for detailed three-way analysis. Reconstructed areas were carefully traced jointly by two experienced operators on the EAM map as the current CARTO® 3 System does not allow simultaneous display of two different 3D reconstructions (Fig. 2). Area measurements were performed using the internal CARTO® 3 System tools. Predefined abnormal tissue categories consisted of low-voltage areas <1.5mV (LowVolt), CMR Scar >3SD (CMR-Sc) and abnormally innervated myocardium <50% tracer uptake (ABNINNERV). This allowed additional myocardial stratification as single-, double- and triple- ischemic structural/functional adaptation (defined as abnormal in one, two, or all three modalities). Regions without complete information in all three modalities were excluded from the analysis.

STATISTICAL ANALYSIS. SPSS (IBM) 16.0 was used for statistical analyses. Continuous variables are expressed as median and quartiles [Q1-Q3] or mean±SD as appropriate. Comparisons between measurements were conducted with a nonparametric Mann–Whitney U test or t-test. Differences were considered significant at a level of $p<0.05$.

RESULTS

EAM AND VT ABLATION. Fifteen patients (

Table 1: Patient Characteristics. Data are presented as mean±SD or n (%). with ischemic cardiomyopathy and drug-refractory VT underwent VT ablation. Detailed EAM was available in all patients with an average LV surface area of 249.5cm^2 [217.5-327.6cm^2] consisting of 653±448 points. All EAMs contained confluent areas of decreased voltage (<1.5mV) consistent with the preexisting ischemic cardiomyopathy. One patient had no inducible VT. In the remaining 14 patients, 46 VTs were inducible with 14 VT representing the clinical/assumed clinical VT. Clinical VTs had a cycle length of 364ms [339-424ms] originating from the interventricular septum (n=2), inferior (n=7), inferoseptal (n=1), lateral (n=2), anterolateral wall (n=1), or apex (n=1), respectively. Post-ablation clinical VTs were no longer inducible with either complete (n=11) or limited PES due to hemodynamic instability (n=3).

TRIPLE MODALITY VISUALIZATION. 3D CMR scar maps were successfully reconstructed from sequential short axis LGE images in all patients using the CARTOSEG™ MR Segmentation Module (10±4 min reconstruction time). Thirteen of the fifteen patients had an Implantable cardioverter-defibrillator in place, which caused a metal artifact affecting 12±10% of the LV surface. Similarly, 3D innervation maps could be generated in all patients based on the short axis ^{123}I-*m*IBG SPECT innervation maps (*8*). Average reconstruction time was 23±8min. Two patients had non-interpretable areas on ^{123}I-*m*IBG SPECT due to increased liver or lung uptake affecting 40% and 37% of the total LV area, respectively.

COMPARISON OF ABNORMAL AREAS. Areas of bipolar voltage less than 1.5mV (LowVolt), CMR scar (CMR-Sc) and abnormal innervation (ABNINNERV) were seen in all patients. The areas of LowVolt, CMR-Sc, and ABNINNERV were 29.5 cm^2 [24.5–102.6 cm^2], 46.1 cm^2 [33.1–86.9 cm^2], 47.8 cm^2 [40.5–68.1 cm^2] in size (Table 2), accounting for 23.3% [17.1–42.0%], 35.1% [22.1–49.5%], 36.6% [26.7–45.0%] out of total analyzable LV area and were similar in size (CMR-

Sc vs ABNINNERV, p=0.44; ABNINNERV vs LowVolt, p=0.09; CMR-Sc vs LowVolt, p=0.23) (Fig. 3).

However, these areas of regional structural and functional adaptation only partially co-localized. The total area of the total VT substrate (TotalVTSubstr) defined as myocardium with any abnormal post-ischemic structural/functional adaptation in at least one of the three categories (LowVolt, CMR-Sc, or ABNINNERV) was 57.6% [52.2-66.1%] of the total analyzable LV area. This was significantly larger (Fig. 3) than any of the three single categories alone (TotalVTSubstr vs CMR-Sc p<0.0001, TotalVTSubstr vs ABNINNERV p<0.0002, TotalVTSubstr vs LowVolt; p<0.0001).

LowVolt, CMR-Sc, and ABNINNERV areas accounted for 49.1% [32.2–73.2%], 58.3% [46.1–81.5%], and 70.6% [52.3–81.0%] of the TotalVTSubstr area, respectively.

The resulting regional heterogeneity of post-ischemic structural and functional adaptation within the total VT substrate is shown in figure 4. The largest component presents that of matching triple-abnormal myocardium (abnormal in all three categories) accounting for 25.2% of the TotalVTSubstr.

However, significant components of the TotalVTSubstr showed abnormalities in only one or two of the categories (single-/double-abnormal; Fig. 4). The largest of these areas consisted of ‘single-abnormal: ABNINNERV only’ (18.2%), ‘double-abnormal: CMR-Sc+ABNINNERV only’ (14.9%) and ‘single-abnormal: CMR-Sc only’ (14.6%).

The areas of single-, double- and triple-abnormal myocardium accounted for 49.3% [29.4–59.7%], 23.3% [19.3–33.1%] and 21.0% [12.4–38.7%] out of TotalVTSubstr area. The single-abnormal area was significantly larger than the double (p=0.010) or triple-abnormal area (p=0.006).

CMR-Sc area overlapped with the areas of the ABNINNERV and LowVolt in 68.3% [41.4%–83.1%] and 59.4% [33.0–86.8%]. ABNINNERV area overlapped with the areas of the CMR-Sc and LowVolt in 61.9% [38.2–83.3%] and 52.3% [24.5–69.9%]. LowVolt area overlapped with the areas of the CMR-Sc and ABNINNERV in 68.3% [38.9–83.3%] and 58.4% [47.0–71.0%].

LOCATION OF ABLATION SITES. All VT channel/exit sites were located within the TotalVTSubstr area demonstrating post-ischemic adaption as shown in figure 5. Additionally, none of the VT channel/exit sites were in an area that showed only abnormalities in one tissue category (CMR-Sc, ABNINNERV or LowVolt), but were all localized within areas of double or triple structural/functional adaptation.

The 'triple-abormal CMR-Sc/ABNINNERV/LowVolt category harbored 12 out of 14 successful ablation sites (86%) and accounted for 11.0% [6.1-18.3%] of the total analyzable LV, 21.0% [12.4-38.7%] of the TotalVTSubstr and 42.8% [20.2-66.0%] of the total CMR-Sc (Fig. 5)**.**

Importantly, all VT channel/exit sites were localized in the 'double-abnormal CMR-Sc/ABNINNERV' category. This double-abnormal area accounted for 16.5% [15.5-32.9%] of the total analyzable LV, 31.2% [25.4-57.2%] of the TotalVTSubstr and 68.3% [41.4-83.1%] of the total CMR-Sc.

Distances of the VT channel/exit sites from closest borders of the CMR-Sc and ABNINNERV zone were 10.9mm [3.2–15.3mm] and 13.0mm [3.4–18.9mm], respectively.

DISCUSSION

This study demonstrated for the first time that (1) structural and functional imaging modalities can be combined to perform multi-modality characterization of the post-ischemic VT substrate; (2) significant regional heterogeneities in structural and functional adaptation exist within the VT substrate; (3) all VT channel/exit sites were within double-abnormal areas of abnormally innervated CMR scar suggesting a proarrhythmic structural and functional adaption within the VT substrate.

CURRENT VT ABLATION APPROACHES. As detailed entrainment/activation mapping without hemodynamic support is only tolerated in 10-30% of cases(*16*), substrate-guided approaches are frequently employed targeting low-voltage areas in conjunction with fractionated signals, late/diastolic potentials, or local abnormal ventricular activity(*17*). However, long-term

ablation success, unfortunately, remains limited with a sustained VT recurrence of 38% after 6 months(*18*).

Structural imaging using either CT or CMR to identify the LV scar by wall thinning or LGE have demonstrated that successful ablation sites were usually located within those structurally abnormal areas(*1,4,10,19,20*). However, areas of structural changes are frequently large (>50cm^2) and well-accepted imaging characteristics identifying the "proarrhythmic" areas within the VT substrate have not been defined conclusively(*1,10,19*).

*RATIONALE FOR COMBINING STRUCTURAL AND FUNCTIONAL VT SUBSTRATE ASSESSMENT.*Myocardial infarction results in tissue necrosis with significant structural and functional adaptation creating a complex proarrhythmic VT substrate. Various histological (fibro-fatty replacement, the presence of fibroblasts/dedifferentiated myofibroblasts) and functional (downregulation/lateralization of connexin 43, reductions of IK_r/IK_s) adaptions point to a diverse process of post-myocardial infarction adaptation (*21*).

Structural imaging with LGE-CMR accurately identifies areas of myocardial scar due to an accumulation of gadolinium in the increased interstitial space(*22*). LGE-CMR-derived 3D maps have been reported to have the potential to assist VT ablation procedures (*1,3,10,19*). However, histologically fibrosis patterns range from homogenous to patchy and to diffuse with a decreasing accuracy to be detected by CMR. Prior studies in ischemic VT comparing CMR scar to EAM have found a good but imperfect correlation with a significant mismatch in up to 1/3 of the patients(*3*) with rather modest correlation with Cohen's κ coefficients ranging from 0.36(*23*) and 0.7(*24*). Indeed, CMR/EAM studies show consistently high scar transmurality points with near preserved voltage(*1,3,10,19*) supporting the notion that bipolar amplitude and CMR determined interstitial fibrosis are closely related but represent two non-identical aspects of the pathophysiological scar remodeling.

Functional imaging is able to assess various cellular adaptations after myocardial infarction, presenting another important, but not an identical aspect of scar remodeling. Autonomic

innervation, a critical component of arrhythmogenesis, can be measured using the radiotracer ^{123}I-*m*IBG(*6,7*). It can provide information about abnormal sympathetic innervation thought to mediate proarrhythmic risk via neurotransmitter accumulation. Indeed, the presence of abnormal cardiac autonomic innervation has been correlated with worsening heart failure outcomes,(*25*) ventricular arrhythmias(*7,8,26,27*) and sudden cardiac arrest(*28*). Damaged myocardial presynaptic nerve terminals demonstrate reduced uptake of catecholamines by the uptake-1 mechanism (*29*) leading to accumulation of neurotransmitters in the synaptic cleft with downregulation of postsynaptic β-adrenergic receptors and an imbalance between pre/postsynaptic signaling favoring proarrhythmia (*30*).

Swine and human studies demonstrated an increased sensitivity of myocardial nerve fibers to ischemia and co-localization of successful VT ablation sites with areas of abnormal innervation even in areas of preserved voltage (*7,29*).

STRUCTURAL AND FUNCTIONAL MULTI-MODALITY IMAGING FOR SUBSTRATE IDENTIFICATION. This suggests that structural as well as functional changes occur as adaptive mechanisms during post-ischemic remodeling. LGE-CMR, myocardial innervation and also myocardial voltage (as another functional measure of myocardial cell integrity) all describe closely-related but different aspects of the complex pathophysiological VT substrate.

This study demonstrates the presence of heterogeneous structural and functional adaptation of the VT substrate. The myocardial area affected by adaptation is larger than predicted by any single modality. Significant areas abnormal in only one or two of the modalities exist in the post-ischemic scar substrate along with triple-abnormal areas demonstrating a complex mixture of post-ischemic myocardial adaptions.

The fibrotic substrate has been proven a critical part of the VT substrate (*31,32*). However, recent high-density mapping studies have demonstrated that functional block is equally important as anatomically fixed block (transmural fibrosis) in sustaining VT (*33*). This implies

that additional functional properties of the not-fully scarred myocardium are an important component of proarrhythmicity.

This study suggests an interplay between structural and functional adaptation in the arrhythmogenesis. Innervation was chosen in this study as swine and human studies supported a direct role and co-localized with successful VT ablation sites (*7,26,29*). The finding of this study that all VT channels/exit sites were located in abnormally innervated CMR scar suggests a possible functional modulation of the anatomic VT substrate. The fact that all ablation sites were in an area of at least two abnormal categories equally raises the question if a certain threshold of adaptation is required to enable proarrhythmicity.

Combining structural and functional assessment may allow identifying more 'proarrhythmic areas' that are more likely to enable VT circuits now and possibly VT recurrences later on.

As such, it may allow for more sophisticated assessment of the VT substrate enabling new pathophysiological insights and novel approaches to imaging-guided VT ablation.

LIMITATIONS

This study represents a small, single-center hypothesis-generating trial and these findings need to be validated by additional and larger studies. Our findings are limited to patients with ischemic cardiomyopathy and will need further assessment in the non-ischemic patient population.

In this study, the well-established n-standard deviation (NSD) method and a 50% ^{123}I-mIBG cut-off derived from prior studies (*7,8*) was used to identify scar in CMR images. Analysis of alternative CMR scar identification algorithms and/or MIBG cut-offs should be included in future studies.

The ^{123}I-mIBG SPECT data were acquired on a SPECT system without an integrated x-ray CT scanner and images were reconstructed without attenuation correction. Abnormally innervated myocardium was assessed visually by two nuclear medicine physicians experienced

in reading SPECT cardiac perfusion scans reconstructed without attenuation correction. Nonetheless, the results of this manuscript should be validated for SPECT/CT systems when attenuation correction is performed.

A careful review of data quality was performed to compensate for differences in spatial resolution (such as mapping density, CMR slice thickness or SPECT camera technology). However, differences in spatial resolution are inherent in any multi-modality imaging study. Similarly, registration errors are difficult to avoid in multi-modality comparisons, but great care was taken during the modality registration to minimize any misregistration by using multiple reviews/reviewers and additional structures like right ventricle or aorta to optimize co-registration.

CONCLUSIONS

Combined structural and functional VT substrate characterization can demonstrate heterogeneities of regional structural and functional post-ischemic remodeling. This provides novel insights into the myocardial adaptations affecting the ischemic VT substrate and its proarrhythmicity. The tissue category of abnormally innervated CMR scar may present a functional/structural state favoring ventricular arrhythmias and enable the identification of novel VT ablation targets.

DISCLOSURES

T.D. – Biosense Webster (Consulting, Grant support), GE (grant support)

V.D. and M.S. – GE (grant support)

R.I. – Biosense Webster (Employee)

K.U., H.I., T.B., J.J., J.D., W.C., M.A., T.S., V.S., A.S., S.S. – no conflicts

ACKNOWLEDGEMENTS

We want to thank Mr. Frank M. Masters and Ms. Elizabeth S. Gault for their continued support and dedication to Electrophysiology Research to improve the life of thousands of patients.

REFERENCES

1. Dickfeld T, Tian J, Ahmad G, et al. MRI-Guided ventricular tachycardia ablation: integration of late gadolinium-enhanced 3D scar in patients with implantable cardioverter-defibrillators. *Circ Arrhythm Electrophysiol.* 2011;4:172-184.

2. Tian J, Jeudy J, Smith MF, et al. Three-dimensional contrast-enhanced multidetector CT for anatomic, dynamic, and perfusion characterization of abnormal myocardium to guide ventricular tachycardia ablations. *Circ Arrhythm Electrophysiol.* 2010;3:496-504.

3. Codreanu A, Odille F, Aliot E, et al. Electroanatomic characterization of post-infarct scars comparison with 3-dimensional myocardial scar reconstruction based on magnetic resonance imaging. *J Am Coll Cardiol.* 2008;52:839-842.

4. Yamashita S, Sacher F, Hooks DA, et al. Myocardial wall thinning predicts transmural substrate in patients with scar-related ventricular tachycardia. *Heart Rhythm.* 2017;14:155-163.

5. Dickfeld T, Lei P, Dilsizian V, et al. Integration of three-dimensional scar maps for ventricular tachycardia ablation with positron emission tomography-computed tomography. *JACC Cardiovasc Imaging.* 2008;1:73-82.

6. Duell J, Dilsizian V, Smith M, Chen W, Dickfeld T. Nuclear imaging guidance for ablation of ventricular arrhythmias. *Curr Cardiol Rep.* 2016;18:19.

7. Klein T, Abdulghani M, Smith M, et al. Three-dimensional 123i-meta-iodobenzylguanidine cardiac innervation maps to assess substrate and successful ablation sites for ventricular tachycardia: Feasibility study for a novel paradigm of innervation imaging. *Circ Arrhythm Electrophysiol.* 2015;8:583-591.

8. Abdulghani M, Duell J, Smith M, et al. Global and regional myocardial innervation before and after ablation of drug-refractory ventricular tachycardia assessed with 123i-mibg. *J Nucl Med.* 2015;56:52S-58S.

9. Tian J, Smith MF, Chinnadurai P, et al. Clinical application of PET/CT fusion imaging for three-dimensional myocardial scar and left ventricular anatomy during ventricular tachycardia ablation. *J Cardiovasc Electrophysiol.* 2009;20:567-604.

10. Wijnmaalen AP, van der Geest RJ, van Huls van Taxis CF, et al. Head-to-head comparison of contrast-enhanced magnetic resonance imaging and electroanatomical voltage mapping to assess post-infarct scar characteristics in patients with ventricular tachycardias: real-time image integration and reversed registration. *Eur Heart J.* 2011;32:104-114.

11. Neilan TG, Coelho-Filho OR, Danik SB, et al. CMR quantification of myocardial scar provides additive prognostic information in nonischemic cardiomyopathy. *JACC Cardiovasc Imaging.* 2013;6:944-954.

12. Yan AT, Shayne AJ, Brown KA, et al. Characterization of the peri-infarct zone by contrast-enhanced cardiac magnetic resonance imaging is a powerful predictor of post-myocardial infarction mortality. *Circulation.* 2006;114:32-39.

13. Komatsu Y, Cochet H, Jadidi A, et al. Regional myocardial wall thinning at multidetector computed tomography correlates to arrhythmogenic substrate in postinfarction ventricular tachycardia: assessment of structural and electrical substrate. *Circ Arrhythm Electrophysiol.* 2013;6:342-350.

14. Bogun F, Good E, Reich S, et al. Isolated potentials during sinus rhythm and pace-mapping within scars as guides for ablation of post-infarction ventricular tachycardia. *J Am Coll Cardiol.* 2006;47:2013-2019.

15. Soejima K, Suzuki M, Maisel WH, et al. Catheter ablation in patients with multiple and unstable ventricular tachycardias after myocardial infarction: short ablation lines guided by reentry circuit isthmuses and sinus rhythm mapping. *Circulation.* 2001;104:664-669.

16. Stevenson WG, Wilber DJ, Natale A, et al. Irrigated radiofrequency catheter ablation guided by electroanatomic mapping for recurrent ventricular tachycardia after myocardial infarction: the multicenter thermocool ventricular tachycardia ablation trial. *Circulation.* 2008;118:2773-2782.

17. Pedersen CT, Kay GN, Kalman J, et al. EHRA/HRS/APHRS expert consensus on ventricular arrhythmias. *Heart Rhythm.* 2014;11:e166-196.

18. Marchlinski FE, Haffajee CI, Beshai JF, et al. Long-term success of irrigated radiofrequency catheter ablation of sustained ventricular tachycardia: Post-approval thermocool vt trial. *J Am Coll Cardiol.* 2016;67:674-683.

19. Desjardins B, Crawford T, Good E, et al. Infarct architecture and characteristics on delayed enhanced magnetic resonance imaging and electroanatomic mapping in patients with postinfarction ventricular arrhythmia. *Heart Rhythm.* 2009;6:644-651.

20. Tian J, Ahmad G, Mesubi O, Jeudy J, Dickfeld T. Three-dimensional delayed-enhanced cardiac MRI reconstructions to guide ventricular tachycardia ablations and assess ablation lesions. *Circ Arrhythm Electrophysiol.* 2012;5:e31-35.

21. Arevalo H, Plank G, Helm P, Halperin H, Trayanova N. Tachycardia in post-infarction hearts: Insights from 3D image-based ventricular models. *PLoS One.* 2013;6:e68872.

22. Kim RJ, Albert TS, Wible JH, et al. Performance of delayed-enhancement magnetic resonance imaging with gadoversetamide contrast for the detection and assessment of myocardial infarction: an international, multicenter, double-blinded, randomized trial. *Circulation.* 2008;117:629-637.

23. Tao Q, Piers SR, Lamb HJ, Zeppenfeld K, van der Geest RJ. Preprocedural magnetic resonance imaging for image-guided catheter ablation of scar-related ventricular tachycardia. *Int J Cardiovasc Imaging.* 2015;31:369-377.

24. Andreu D, Berruezo A, Ortiz-Pérez J, et al. Integration of 3D electroanatomic maps and magnetic resonance scar characterization into the navigation system to guide ventricular tachycardia ablation. *Circ Arrhythm Electrophysiol.* 2011;4:674-683.

25. Jacobson AF, Senior R, Cerqueira MD, et al. Myocardial iodine-123 meta-iodobenzylguanidine imaging and cardiac events in heart failure. Results of the prospective ADMIRE-HF (AdreView Myocardial Imaging for Risk Evaluation in Heart Failure) study. *J Am Coll Cardiol.* 2010;55:2212-2221.

26. Klein T, Dilsizian V, Cao Q, Chen W, Dickfeld T. The potential role of iodine-123 metaiodobenzylguanidine imaging for identifying sustained ventricular tachycardia in patients with cardiomyopathy. *Curr Cardiol Rep.* 2013;15:359.

27. Boogers MJ, Borleffs CJ, Henneman MM, et al. Cardiac sympathetic denervation assessed with 123-iodine metaiodobenzylguanidine imaging predicts ventricular arrhythmias in implantable cardioverter-defibrillator patients. *J Am Coll Cardiol.* 2010;55:2769–2777.

28. Fallavollita JA, Heavey BM, Luisi AJ, Jr., et al. Regional myocardial sympathetic denervation predicts the risk of sudden cardiac arrest in ischemic cardiomyopathy. *J Am Coll Cardiol.* 2014;63:141-149.

29. Sasano T, Abraham MR, Chang KC, et al. Abnormal sympathetic innervation of viable myocardium and the substrate of ventricular tachycardia after myocardial infarction. *J Am Coll Cardiol.* 2008;51:2266-2275.

30. Caldwell JH, Link JM, Levy WC, Poole JE, Stratton JR. Evidence for pre- to postsynaptic mismatch of the cardiac sympathetic nervous system in ischemic congestive heart failure. *J Nucl Med.* 2008;49:234-241.

31. de Bakker JM, van Capelle FJ, Janse MJ, et al. Slow conduction in the infarcted human heart. 'Zigzag' course of activation. *Circulation.* 1993;88:915-926.

32. Stevenson WG, Khan H, Sager P, et al. Identification of reentry circuit sites during catheter mapping and radiofrequency ablation of ventricular tachycardia late after myocardial infarction. *Circulation.* 1993;88:1647-1670.

33. Tschabrunn CM, Roujol S, Nezafat R, et al. A swine model of infarct-related reentrant ventricular tachycardia: Electroanatomic, magnetic resonance, and histopathological characterization. *Heart Rhythm.* 2016;13:262-273.

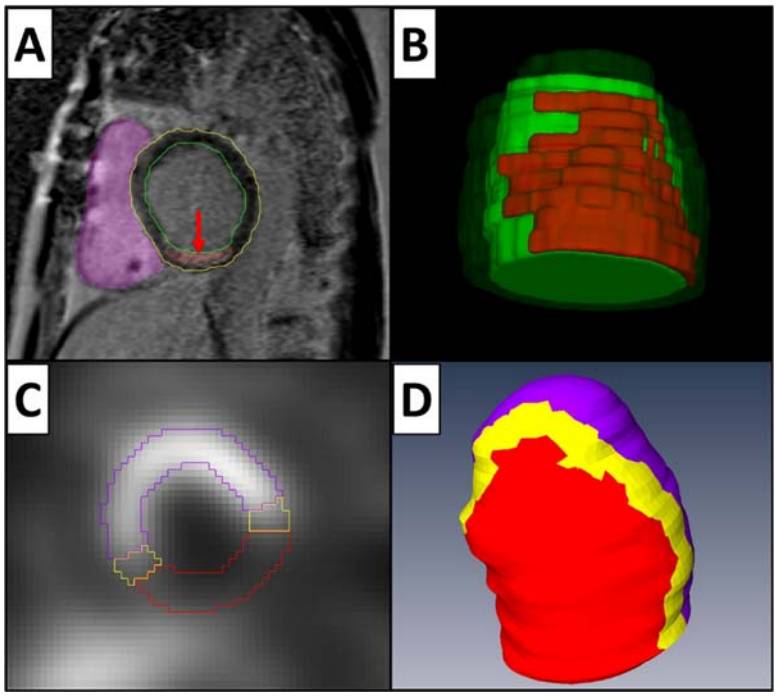

Figure 1

LGE-CMR and ^{123}I-*m*IBG SPECT Reconstruction: **A.** Epicardial (yellow line) and endocardial (green line) borders of the Left ventricle outlined by manual segmentation of the short-axis LGE-CMR slices. Right ventricle (purple) reconstruction used to minimize rotational errors during registration. Scar reconstruction based on the voxel intensity (red arrow). **B.** 3D reconstruction of the myocardial scar (red) embedded in myocardial reconstruction (green). **C.** ^{123}I-*m*IBG SPECT short-axis slice demonstrating the lack of uptake in the infero-lateral wall consistent with abnormal innervation. **D.** 3D reconstruction of ^{123}I-*m*IBG SPECT–derived innervation map with inferior view demonstrating normally innervated (purple), abnormally innervated (red, <50% uptake) and transition zone (yellow) myocardium.

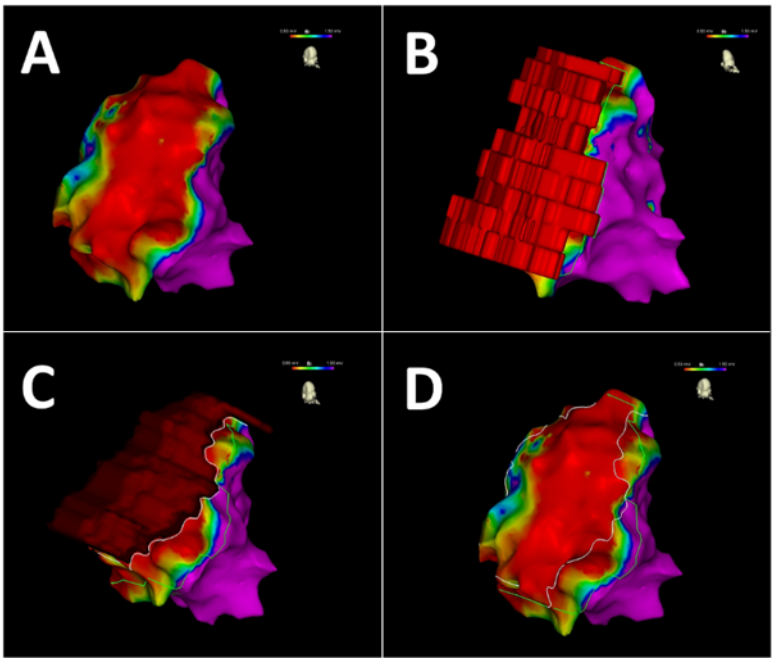

Figure 2

Comparison of 3D LGE-CMR map, ^{123}I-*m*IBG SPECT innervation map and electroanatomic map (EAM). **A.** Bipolar EAM, inferior view, demonstrating inferior scar (red, <0.5mV), border zone (yellow-blue, 0.5-1.5mV) and normal voltage (purple, >1.5mV). **B.** Co-registration of EAM and LGE-CMR map. Green line demonstrates projected border of the CMR Scar (CMR-Sc). **C.** Co-registration of EAM map and ^{123}I-*m*IBG SPECT innervation map. White line demonstrates projected border of abnormal innervation zone (ABNINNERV). **D.** EAM with green and white lines (see B and C) corresponding to the borders of abnormal myocardial areas. *Note mild rotational changes in B and C demonstrating perpendicular view used to trace accurately the contours of the CMR and innervation reconstruction.*

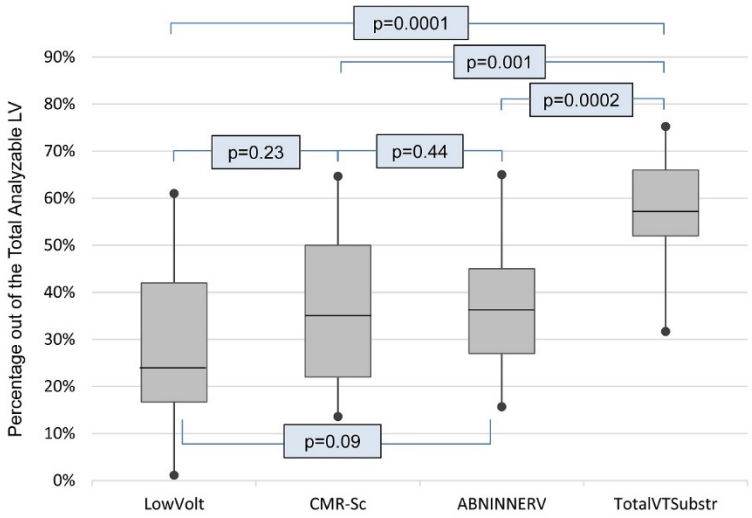

Figure 3

Graph showing the percentages of the EAM low-voltage (LowVolt, <1.5 mV), LGE-CMR scar (CMR-Sc), ^{123}I-*m*IBG SPECT abnormal innervation (ABNINNERV) areas and total VT substrate area with an abnormal area in at least one imaging modality (TotalVTSubstr) out of the total analyzable LV area.

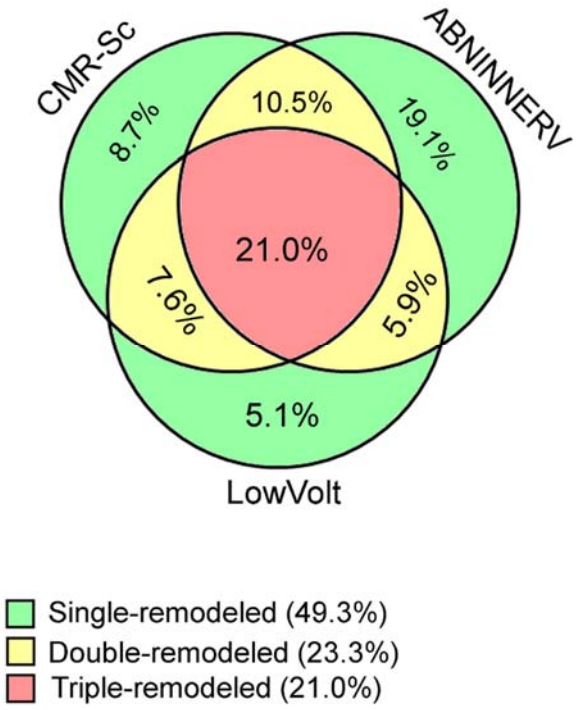

Figure 4

Comparison of abnormal areas. CMR-Sc: scar defined by LGE-CMR (>3SD). LowVolt: area of low-voltage (<1.5mV). ABNINNERV: abnormally innervated area of the left ventricle by ^{123}I-*m*IBG SPECT (<50% tracer uptake). Green: single-abnormal, yellow: double-abnormal, red: triple-abnormal area. The numbers represent the median percentage of a given area out of the total VT substrate area.

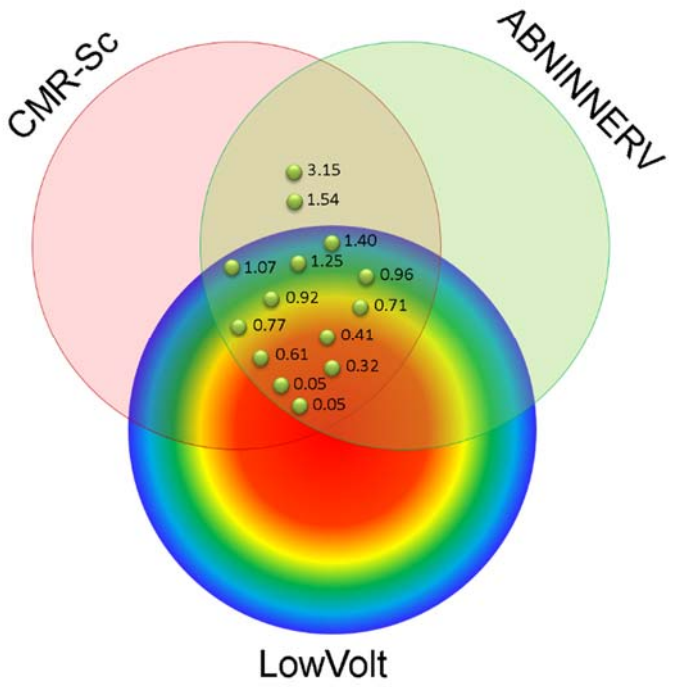

Figure 5

Successful VT Channel/Exit Site Location in reference to CMR-Sc (CMR scar), LowVolt (area <1.5 mV) and ABNINNERV (abnormal innervation, <50% tracer uptake). The different colors further stratify the EAM LVA according to voltage. Each green point represents a VT channel/exit site according to local bipolar voltage.

TABLES

Characteristics	Values
Sex, male	13 (87%)
Age at time of ablation	71.2±7.7
Ejection Fraction	28±10%
Presence of ICD at time of ablation	13 (87%)
Comorbidities	
Diabetes Mellitus	2 (13%)
Hypertension	10 (67%)
Hyperlipidemia	6 (40%)
Atrial fibrillation	4 (27%)
Congestive Heart Failure	6 (40%)
Medications	
Beta-blocker	15 (100%)
ACEI/ARB	13 (87%)
Amiodarone	9 (60%)
Aldosterone antagonist	1 (7%)
Other antiarrhythmic drugs	0 (0%)

ICD, Implantable cardioverter defibrillator; ACEI, Angiotensin converting enzyme inhibitor; ARB, Angiotensin receptor blocker

Table 1: Patient Characteristics. Data are presented as mean±SD or n (%).

	Area size (cm^2)	Percentages out of the total VT substrate
CMR-Sc*s	46.1 [33.1-86.9]	58.3 [46.1-81.5]
ABNINNERV*	47.8 [40.5-68.1]	70.6 [52.3-81.0]
LowVolt*	29.5 [24.5-102.6]	49.1 [32.2-73.2]
Sum of all single-abnormal areas	29.0 [18.5-87.2]	49.3 [29.4-59.7]
Sum of all double-abnormal areas	25.7 [12.6-34.0]	23.3 [19.3-33.1]
Triple-abnormal area	15.1 [9.9-38.2]	21.0 [12.4-38.7]
TotalVTSubstr	76.0 [57.9-143.2]	100

***CMR-Sc**: scar defined by LGE-CMR (>3SD). **LowVolt**: area of low-voltage (<1.5mV) **ABNINNERV**: abnormal innervation (<50% tracer uptake); **TotalVTSubstr**: total VT substrate area with an abnormal area in at least one imaging modality.

Table 2: Imaging Characteristics. Continuous variables are expressed as median and quartiles [Q1–Q3] *(Note: as results expressed in median, sum of single-/double-/triple-abnormal area is not exactly 100%).*